Journal of ASTM International, Vol. 4, No. 8
Paper ID JAI100743
Available online at www.astm.org

D. Kaoumi,[1] *A. T. Motta,*[1] *and R. C. Birtcher*[2]

Grain Growth in Nanocrystalline Metal Thin Films under *In Situ* Ion-Beam Irradiation

ABSTRACT: In-situ observations in a transmission electron microscope (TEM) were used to study the microstructure evolution in metal Zr, Pt, Cu, and Au nanocrystalline thin films under ion-beam irradiation. Free-standing films were prepared by sputter deposition. Samples were irradiated in-situ at the Intermediate Voltage Electron Microscope (IVEM) at Argonne National Laboratory with Ar and Kr ions to fluences in excess of 10^{16} ion/cm^2. As a result of irradiation, grain growth was observed in all samples using Bright Field (BF) imaging in the TEM. The average grain size increased monotonically with ion fluence until it reached a saturation value. Similarly to thermal grain growth, the ion-irradiation induced grain growth curves could be best fitted with curves of the type: $D^n-D_0^n=K\Phi$. The irradiations were done at temperatures ranging from 20 to 773 K. The results suggest the existence of three regimes with respect to irradiating temperature: (i) a purely thermal regime, which appears to start above the bulk coarse-grained recrystallization temperature, (ii) a thermally assisted regime where thermal diffusion and irradiation effects combine to increase the rate of grain growth relative to that resulting from either of these mechanisms alone, and (iii) an athermal regime (low-temperature regime) where irradiation can by itself cause grain growth. The transition temperature between the athermal regime and the thermally assisted regime depends on the material, but is in the range 0.14–0.22 times the melting point. The influence of the ion type was also investigated on Zr-Fe irradiated with 600 keV Kr ions versus 600 keV Ar ions.

KEYWORDS: ion beam irradiation, grain growth, thin film, in-situ, TEM, nanocrystalline

Introduction

Ion-irradiation induced grain growth has been observed and investigated in different pure metals and alloy systems [1–9]. However, there have been few systematic studies of the phenomenon, and most were performed at room temperature or higher. Also, most of these studies were based on results observed after irradiation, i.e., an irradiation dose is applied to the material from which a TEM sample is subsequently prepared to study grain growth. Given the dynamical nature of the phenomenon, a direct observation of ion-irradiation induced grain growth is very beneficial for better understanding the mechanism, kinetics and driving force of this process.

In the present work, a systematic study of ion-irradiation induced grain growth in sputter-deposited elemental thin films of Zr, Cu, Pt, and Au, and supersaturated solid solutions of Zr-Fe has been carried out in-situ at the Intermediate Voltage Electron Microscope (IVEM) (Hitachi H9000NAR) facility at Argonne National Laboratory. The irradiations were performed over a large range of temperatures (50–573 K). We present the experimental results of this investigation of ion-irradiation induced grain growth including the dependence of grain growth on ion dose, irradiating temperature, ion type.

Experimental Methods

Materials and Sample Preparation

Elemental thin films of Zr, Cu, Pt, and Au, and supersaturated solid solutions of Zr-Fe were (co-)sputter deposited onto NaCl substrates and onto Si wafers (for Rutherford Backscattering Spectroscopy (RBS)

Manuscript received August 3, 2006; accepted for publication July 22, 2007; published online September 2007. Presented at ASTM Symposium on Effects of Radiation on Materials: 23rd Symposium on 13–15 June 2006 in San Jose, CA; R. Lott, Guest Editor.

[1] Graduate Researcher and Professor, Department of Mechanical and Nuclear Engineering, 227 Reber Bldg., Pennsylvania State University, State College, PA 16802.

[2] Principal Investigator, Materials Science Division, Bldg. 212Argonne National Laboratory, Argonne, IL 60540.

TABLE 1—*Characteristics of as-deposited films.*

Composition	Crystal Structure observed	Target Film Thickness (nm)	Initial Grain-size (nm) (± error in nm)
Au	fcc	80	12 (1.2)
Pt	fcc	80	13 (2.4)
Cu	fcc	90	13 (1.4)
Zr	hcp	80	14 (1.8)
Zr(Fe)	hcp	80	14 (1.6)

characterization) using a dual gun system at a base pressure of less than 10^{-6} torr at room temperature at the Materials Research Laboratory (MRL), Penn State University. The coated NaCl substrates were then cleaved into small pieces and the specimens were floated on a deionized water-ethanol solution onto TEM copper grids, cleaned in deionized water, and dried before they were used in the IVEM.

The four elements were chosen to independently investigate the role of collisional processes and melting temperature: Pt and Zr have similar melting points but very different atomic masses (i.e., different recoil spectra); and the same is true for Au and Cu. On the other hand, Pt and Au are adjacent elements in the periodic table of elements and should therefore have similar collisional behavior under the same irradiation conditions, but the two elements have very different melting points, hence comparing results for both elements should highlight the role of melting temperatures of the elements on the grain growth process. Also, both Pt and Au are noble metals and are expected to be resistant to chemical reactions which may occur under thermal heating or irradiation; one does not need to worry about possible oxidation. The crystal structure of Au, Cu, and Pt is face-centered cubic (fcc), in contrast with Zr which is hexagonal-close packed (hcp).

Microstructure of As-deposited Films

Film thickness and deposition rates were measured with a thickness profilometer. Deposition rates varied depending on the metal but were usually between 0.1–1.0 nm/s. The films used in this study were between 80–90-nm thick. One set of Au samples was processed with a thickness of about 50 nm in order to determine the effect of film thickness in the grain growth experiments. The thickness and composition of the films deposited onto Si pieces was examined using Rutherford Backscattering Spectrometry (RBS). Elemental composition analysis was also performed by X-ray dispersive spectroscopy in an ESEM (FEI Quanta 200 ESEM) equipped with an energy dispersive X-ray (EDS) system.

The as-deposited films are laterally homogeneous, and nanocrystalline, with an initial mean grain size between 10 and 15 nm, as shown in Table 1. They have a more or less equiaxed grain microstructure. However no cross-sectional examinations were performed. Figure 1 shows bright-field electron transmission electron micrographs of the as-deposited elemental Au, Pt, and Cu films. The diffraction patterns of the as-deposited films were characteristic of Cu, Au, Pt, respectively, with the expected fcc crystal structures (hcp in the case of Zr) and with lattice parameters equal to those of the bulk materials. For the Zr-Fe solid solutions only the diffraction pattern of hcp-Zr, respectively, were observed.

Grain size was determined by measuring the grains on the TEM bright-field micrographs; the grain size was averaged over the number of grains measured; the initial average grain size was determined for each sample used for each irradiation experiment; hence, the error reported in Table 1 is a combination of the error associated with the measurements (typically ±1 nm) and the spread of average grain-size values from sample to sample (or area to area of the sample).

Irradiation Experiments

The ion irradiations were conducted at the Intermediate Voltage Electron Microscope (IVEM)-TANDEM facility at Argonne National Laboratory, where an ion accelerator is attached to an electron microscope operated at 300 keV [10] so that the grain growth (and the qualitative evolution of grain morphology) could be followed in-situ on the microscope. Samples were irradiated with 500 keV Ar and Kr ions, 600 keV Ar and Kr ions, and with 1 MeV Kr ions at different temperatures ranging from 20 K to 573 K. The ion-beam energy was chosen on the basis of computer simulations using the Monte Carlo program SRIM2003 so as to minimize ion implantation while maximizing the deposited damage energy [11]. The

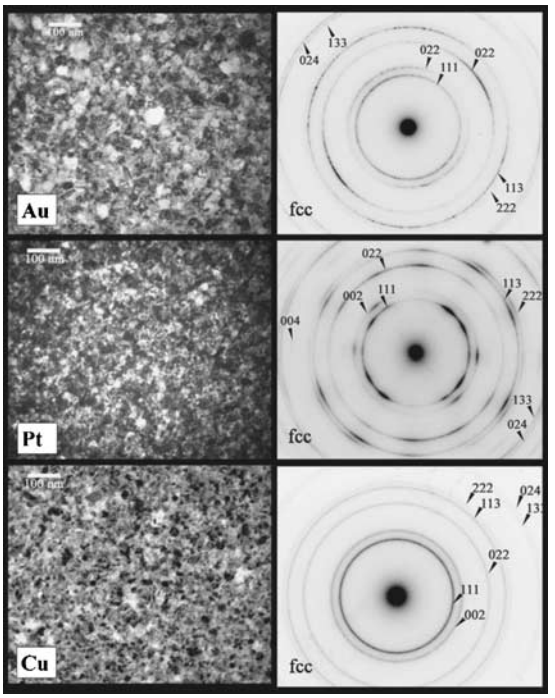

FIG. 1—*Bright field micrographs and associated diffraction patterns of as-deposited Au, Pt, and Cu films. The diffraction rings are indexed using only the phases shown in Table 1.*

energy of the ions was such that most ions (typically between 84 and 98 %) pass through the samples for the different cases. The greatest implantation would occur in 500 keV Kr in 900 A thick Cu thin films, and in that case 67 % of the ions pass through. Ion fluxes were typically around 2.50×10^{12} ions/cm^2-s. The irradiation conditions such as ion type and energy, melting points of the materials, and the collisional properties (displacement rate and deposited damage-energy F_D) are summarized in Table 2.

Geometry of the System

Figure 2 shows schematically the geometry of the system. The angle between the incident electrons and the ion beam was 30°. The sample was tilted from the flat position with respect to the electron beam and held with an inclination angle of 15° with respect to the ion beam. Due to the geometry of the system illustrated in Fig. 2 some regions of the sample were systematically shadowed by the thickness of the TEM grid, and, hence, not irradiated by the beam. The microstructure evolution in these regions revealed the thermal effects alone, while the irradiated areas revealed the impact of both temperature and irradiation. Thus the nonirradiated regions provide a built-in control to separate the purely thermal effects from those that require irradiation. To further understand the thermal effects on grain growth, selected isothermal runs were also performed on some samples without irradiation.

The evolution of the microstructure was followed by sequentially taking bright-field images and diffraction patterns (DP) of the films while they were being irradiated. This made it possible to follow the kinetics of the irradiation induced phenomena.

TABLE 2—*Summary of the irradiation conditions: melting points, ion type and energy, and collisional properties (displacement rate and deposited damage-energy F_D) obtained from the SRIM2003 [11] Monte-Carlo code using a displacement energy of 25 eV.*

Element	Melting Point (K)	Ion Type/Energy	Damage Deposited Energy (F_D) (eV/ion-Å)	# Displacements/Ion-Å	Displacement Rate (dpa/s)
Au	1337	Ar 500 keV	100	2.83	0.012
Pt	2041	Ar 500 keV	120	3.50	0.013
		Kr 1 MeV	367	9.78	0.018
Cu	1358	Kr 500 keV	323	7.91	0.023
Zr	2128	Kr 500 keV	194	3.67	0.021

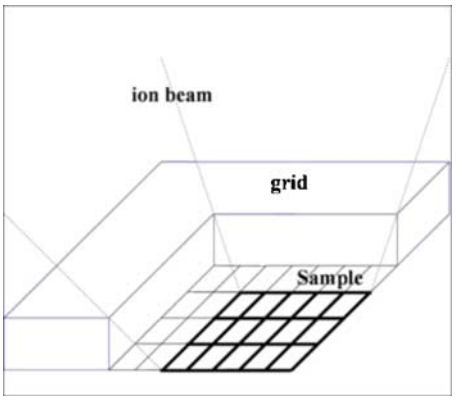

FIG. 2—*Schematic sample configuration showing the irradiated sample area (dark) and the unirradiated area (light).*

Results

In-situ Observation of Ion-irradiation Induced Grain Growth

Direct observation of the films under irradiation revealed a dynamic picture of the phenomenon of ion-irradiation induced grain growth, i.e., a gradual increase of the average grain size (i.e., average grain diameter). Grain growth occurred for all ion energies, and all irradiation temperatures examined, even below 50 K where thermal diffusion should be very small.

Figure 3 shows a sequence of bright field pictures of different elemental films irradiated at room temperature taken at different ion fluences. The Pt and Au samples shown were irradiated with 500 keV Ar ions and the Cu sample was irradiated with 500 keV Kr ions. The increase of grain size is apparent on the micrographs. The grain growth in Au and Cu is much more extensive than for Pt, at a given fluence. In fact

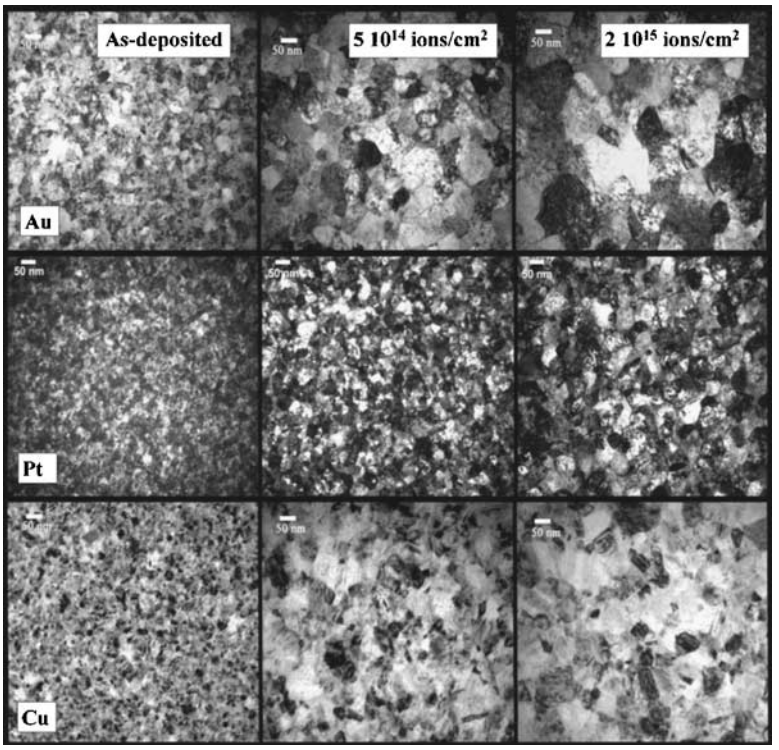

FIG. 3—*Sequence of bright-field images taken at different ion doses showing grain growth induced by ion-irradiation (from left to right: as deposited, 5×10^{14} ions/cm^2, 2×10^{15} ions/cm^2). From top to bottom: pure Au and Pt thin-films both irradiated with 500 keV Ar ions and Cu thin film irradiated with 500 keV Kr ions at room temperature.*

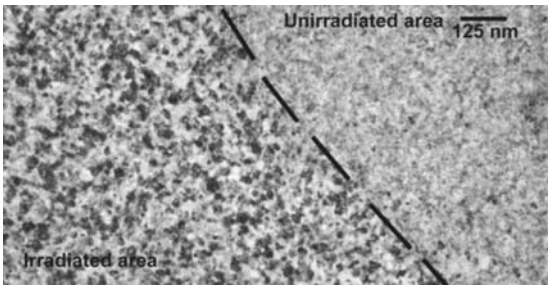

FIG. 4—*Bright-field micrograph of the interface between the irradiated (left) and unirradiated (right) regions in a Zr-1.2 %Fe film irradiated with 600 keV Kr ions at an ion fluence of 10^{16} ions/cm^2 at 573 K.*

at the last fluence, the average grain diameter for Au and Cu far exceeds the thickness of the foil. In parallel, the diffraction patterns became spottier as the fluence increased, also indicating grain size increase. Ion-irradiation induced grain growth was observed to be laterally uniform (relatively narrow range of grain size) at all doses examined. No secondary or abnormal grain growth was observed.

During the early part of the irradiation a small amount of grain recrystallization occurred that eliminated some amorphous-like structure in the as-deposited films, which was detected by the diffuse diffraction rings in the initial diffraction patterns; these diffraction rings became sharper and the grains more visible under irradiation. This was particularly noticeable for some Zr films which seemed to start more amorphous.

We note that the observed grain growth does not result from ion-beam heating. Calculations based on a simple heat conduction model showed that in the given configuration, with the sample holder in contact with the grid, itself in total contact with the sample, the temperature rise in the sample is less than 10 K for the ion fluxes used. This increase is negligible in terms of thermal activation processes involved in thermal grain growth.

Furthermore, the areas shadowed by the grid experienced little, if any changes in grain size. Figure 4 shows the limit between the irradiated area and the nonirradiated area (shadowed by the grid as shown in Fig. 2) in a Zr-1.2%Fe sample irradiated with 600 keV Kr ions at the irradiating temperature of 573 K. There is a sharp demarcation line of the two regions: grains are clearly much bigger in the irradiated area. Grain growth did not occur in the nonirradiated area which was held at 573 K for the time of the experiment (about 2.5 h). If beam heating were to play a major role in the grain growth process, the effects should be noticeable in the unirradiated area as well due to thermal conductivity in the metal films.

The absence of grain growth in the unirradiated area indicates the lack of influence of beam heating in the grain growth process. Similar conclusions where drawn by Wang in his study of Ni films irradiated with Ag ions [1,12] and by Atwater [7] who concluded that if beam heating were to influence grain growth, then changing the beam flux should have a noticeable impact on the grain growth, which he did not observe after changing the ion beam flux by a factor of 10.

Thermal Grain Growth

To further investigate the role of temperature, purely thermal runs were conducted for selected samples at the Materials Research Laboratory (at PSU) using a Philips 420 TEM operated at 120 kV. In these runs the sample was held at a fixed temperature in a heating sample-holder similar to the one used at Argonne Laboratory. Thin films of Cu, Au, and Pt exhibited grain growth by 0.38 T_m. For Zr thin films held at annealing temperatures up to 873 K (0.41 T_m), grain growth was not observed during the observation time (up to 6 h). The only noticeable phenomenon occurring during these runs was the crystallization of some of the samples which were initially somewhat amorphous, during the early stages of irradiation as mentioned above.

Grain Size Measurements

The bright field TEM micrographs served as the basis to find the average grain size at the different fluences. In a given micrograph, the grain size was calculated as the average of the smaller and larger diameter of each grain, and then averaged over as many grains as were discernible on the micrograph

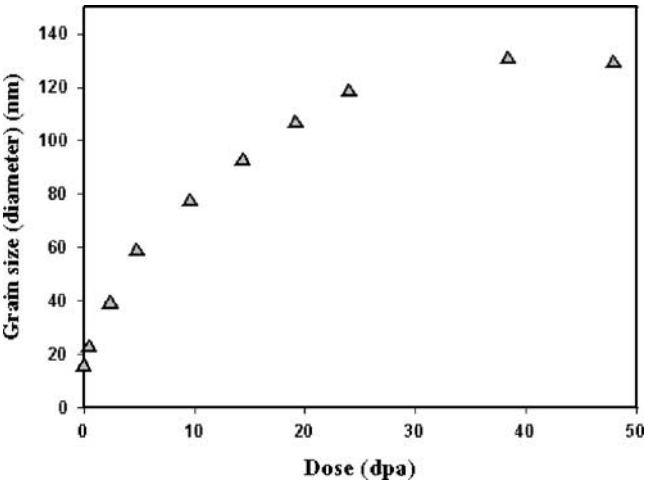

FIG. 5—*Average grain size in Au film irradiated in situ at room temperature with 500 keV Ar ions plotted versus dose in dpa.*

(typically between 30 and 80 grains, less at higher fluences after the grains have grown). The average grain size in the metal films was then plotted versus ion dose for the different ions and irradiating temperatures. In order to compare the grain growth kinetics between different materials, it is more meaningful to plot the average grain size and other properties as a function of the number of displacement per atom (dpa) rather than the ion fluence (ions/cm^2). The estimation of the number of dpa was made using the Monte-Carlo code SRIM2003 which calculates displacement cross sections for ions interacting with matter [11], as reported in Table 2.

The grain growth curves revealed a common trend for all compositions considered and for all irradiating temperatures: grain size increases gradually and monotonically (but at ever decreasing rates) with ion dose until it reaches saturation. As an example, Fig. 5 shows the average grain diameter of an Au film irradiated in-situ with 500 keV Ar ions plotted as a function of ion dose in dpa. Similarly to the relationship between the average grain size (D) and annealing time (t) in the case of thermally induced grain growth [13,14] ion-irradiation induced grain growth curves can be fitted with the expression: $D^n - D_0^n = K\Phi$ where $\boldsymbol{D}_0$ is the initial mean grain diameter, $\boldsymbol{\Phi}$ is the ion dose, $\boldsymbol{n}$ is a constant and $\boldsymbol{K}$ is proportional to the grain boundary mobility of the material and the driving force. The curve fittings were determined according to the expression given above using DataFit 9.0 software by Oakdale Engineering to perform the least-squares fit. The fitting parameters (K, n) varied depending on the material and the temperature. The n value is found between 2.5 and 4.5 revealing a slower grain growth than predicted by Hillert's model of grain growth driven by grain curvature for which $n=2$ [15].

Role of Ion Type

In order to determine the influence of the projectile mass, Zr-Fe films were irradiated at 573 K with both 600 keV Ar ions and 600 keV Kr ions. Table 3 summarizes the main experimental parameters of these irradiations.

Figure 6 shows the average grain size in the Zr-Fe films irradiated at 573 K with 600 keV Ar ions and 600 keV Kr ions versus ion fluence (ions/cm^2). At a given fluence grain growth is more pronounced for 600-keV-Kr ion irradiation than for 600-keV-Ar ion irradiation. The final grain size in the saturation regime also appears to be larger under Kr irradiation than Ar ion irradiation.

TABLE 3—*Irradiation parameters for 80 nm Zr slab irradiated with both 600 keV Ar ions and 600 keV Kr ions at 573 K.*

Ion Type/Energy	Atomic Mass	Damage Energy Deposited (eV/ion- Å)	Displacement Cross Section (#disp/ion-Å)	Displacement Rate (dpa/s)
Ar 600 keV	40	40.9	0.82	0.004
Kr 600 keV	83.8	180	3.25	0.019

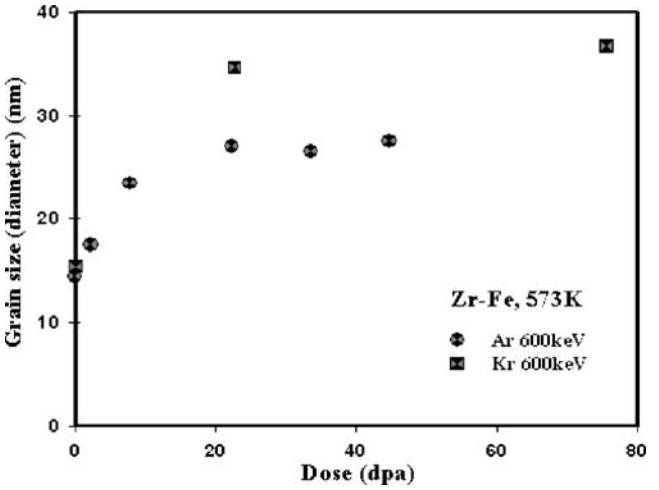

FIG. 6—*Average grain size in Zr-Fe films irradiated in-situ at 573 K with 600 keV Ar and 600 keV Kr ions versus the dose in dpa.*

Role of Irradiation Temperature

Figure 7 shows the average grain size for various Zr-Fe supersaturated alloys irradiated with 500 keV Kr ions at different temperatures. The measured grain sizes in samples irradiated at 20 K and at 293 K are very similar. At higher temperatures, both the rate of grain growth and the final saturation grain size increase with irradiation temperature. The results suggest the existence of three regimes with respect to irradiating temperature: a low-temperature regime where the kinetics of ion-irradiation induced grain growth are independent of temperature, an intermediate-temperature range where grain growth kinetics are affected by both temperature and irradiation and a higher temperature where thermal effects dominate.

The same conclusions can be drawn from the case of Pt films irradiated with 1 MeV Kr ions at different temperatures as shown in Fig. 8. Indeed, the grain growth curves for the irradiations conducted at room temperature and 50 K are also similar, and an increase in grain growth kinetics is seen for higher irradiation temperature similarly to the case of Zr-Fe.

The grain-growth curves for Pt and Zr (Figs. 7 and 8) indicate that the transition temperature from temperature-independent regime to temperature dependent regime for these elements is above room temperature (since there seems to be little difference between the grain growth curves for both elements at 50 K and at room temperatures). In the case of Au and Cu, grain growth curves were also plotted at various temperatures as shown in Figs. 9 and 10. Clearly grain growth is enhanced at room temperature

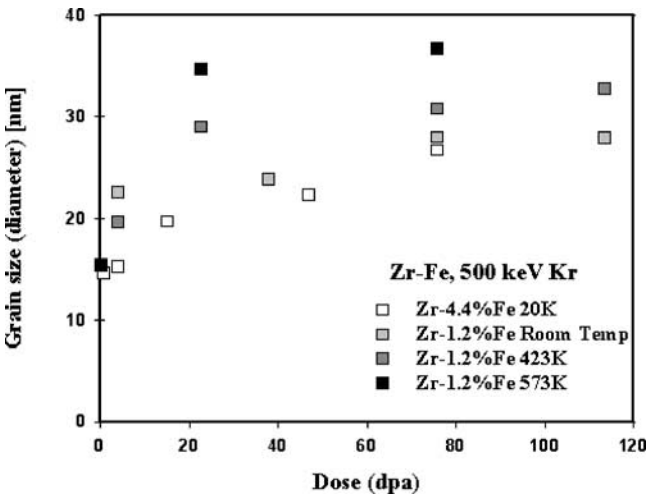

FIG. 7—*Average grain size in Zr-1.2 %Fe thin foils irradiated in-situ with 500 keV Kr ions plotted versus the dose in dpa for different temperatures [16]. This plot highlights the effect of irradiation temperature on ion beam induced grain growth in the Zr-Fe thin films.*

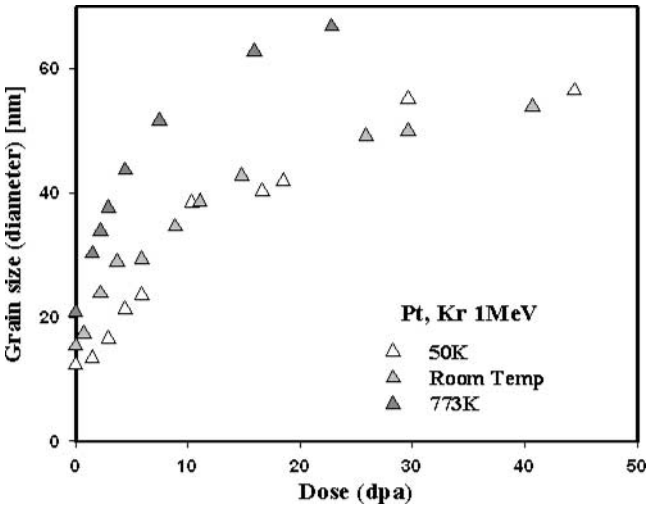

FIG. 8—*Effect of irradiation temperature on ion beam induced grain growth in Pt thin films irradiated with 1 MeV Kr ions. Average grain size is plotted versus the dose in dpa for different irradiating temperatures.*

compared with the cryogenic run, which suggests that for Au and Cu the transition temperature between the two regimes is below room temperature. A temperature dependence was also noted in Cu thin films irradiated with Ar^{+} and Xe^{++} at temperatures above 213 K [5] but in that study, the films were irradiated to a single fluence.

Role of Intrinsic Material Properties

Since in the low-temperature regime, grain growth kinetics are independent of the substrate temperature, a legitimate question is whether ion-irradiation-induced grain growth in this regime is not purely collisional. If this is the case, then materials with similar collisional properties (i.e., damage energy linear density F_D and recoil energy spectra) should exhibit similar grain growth kinetics. If this is not the case than materials properties must be affecting grain growth and therefore they should be taken into account in the model. Au (atomic mass=196.97) and Pt (atomic mass=195.08) are adjacent elements in the periodic table of elements and SRIM calculations show that they have similar recoil energy spectra under the same irradiation conditions. However they have very different melting points, thermal conductivities, cohesive

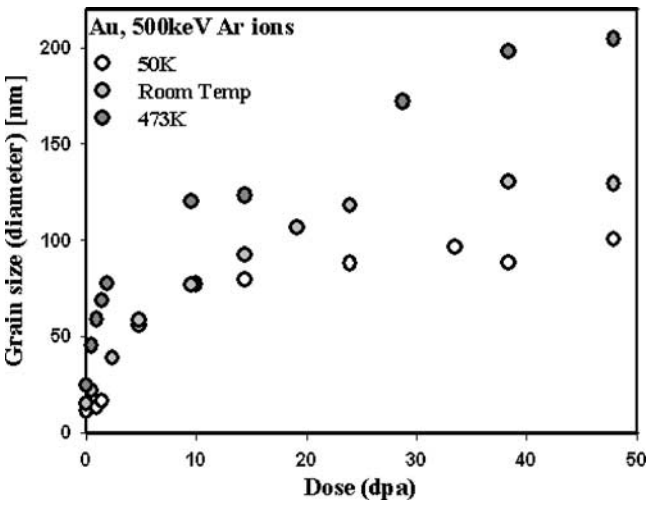

FIG. 9—*Effect of irradiation temperature on ion beam induced grain growth in Au thin films irradiated with 500 keV Ar ions. Average grain size is plotted versus the dose in dpa for different irradiating temperatures.*

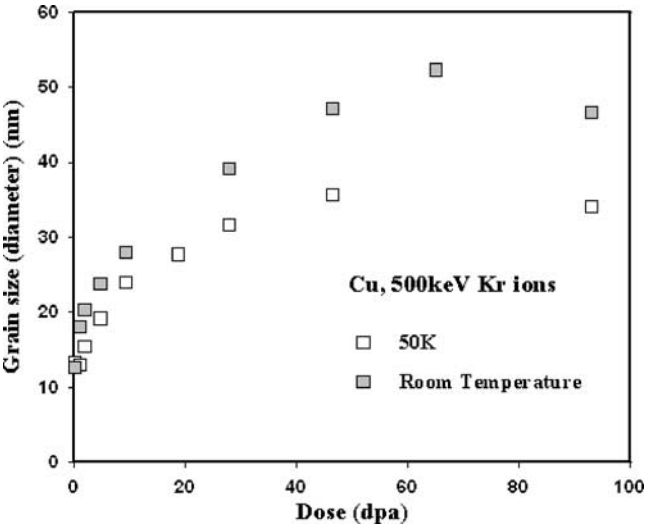

FIG. 10—*Effect of irradiation temperature on ion beam induced grain growth in Cu thin films irradiated with 500 keV Kr ions. Average grain size is plotted versus the dose in dpa for different irradiating temperatures.*

energies (i.e., atomic jump activation energies) as shown in Table 4. As a consequence, by comparing their grain growth kinetics under similar irradiation conditions we can highlight the specific influence of these material properties on grain-growth.

Figure 11 shows the average grain size plotted versus ion dose for Pt and Au films both irradiated with 500 keV Ar ions in the low-temperature regime where the kinetics of grain growth are independent of temperature. Grain growth is more than two times larger in the Au films than in the Pt films although both materials were irradiated in similar experimental conditions (same temperature and same ion type/energy). Since the recoil spectra are quite similar, this means that intrinsic properties of the materials must play a determining role in the grain growth kinetics. In other words, collisional properties (such as the deposited damage energy and recoil spectra) cannot explain alone grain growth kinetics and any attempt to model the phenomenon should account for those intrinsic properties of the material.

Discussion

In this work we completed our study of ion-irradiation induced grain growth which started with the Zr-Fe system [16] with irradiations of Pt, Au, Cu, thin films carried out at temperatures varying from 50 K to 773 K depending on the material. Significant grain growth was observed in all the samples studied.

Based on this, we can identify three temperature regimes for grain growth in nanostructured thin films under irradiation:

(i) a purely thermal regime, which appears to start above the bulk recrystallization temperature,
(ii) a thermally-assisted regime where thermal motion and irradiation effects combine to increase the rate of grain growth caused by either of these mechanisms operating alone, and
(iii) a low temperature (or "athermal") regime in which ballistic effects of ion irradiation dominate the grain growth process.

TABLE 4—*Intrinsic properties of Pt and Au and their collisional characteristic obtained from SRIM2003 code for simulations of irradiations of 80-nm thick films irradiated with 500 keV ions with an incidence angle of 15 deg.*

Element	Structure at Room Temperature	Atomic Mass (amu)	Atomic Density (10^{22} cm^{-3})	ΔH_{coh} (eV/at)	Melting Point (K)	Ion Type/ Energy	Deposited Damage-energy (eV/ion-Å)	Displacement Rate (dpa/sec)
Pt	Fcc	195.08	6.60	5.84	2041	Ar 500 keV	120	0.0128
Au	Fcc	196.97	5.90	3.81	1337	Ar 500 keV	100	0.0119

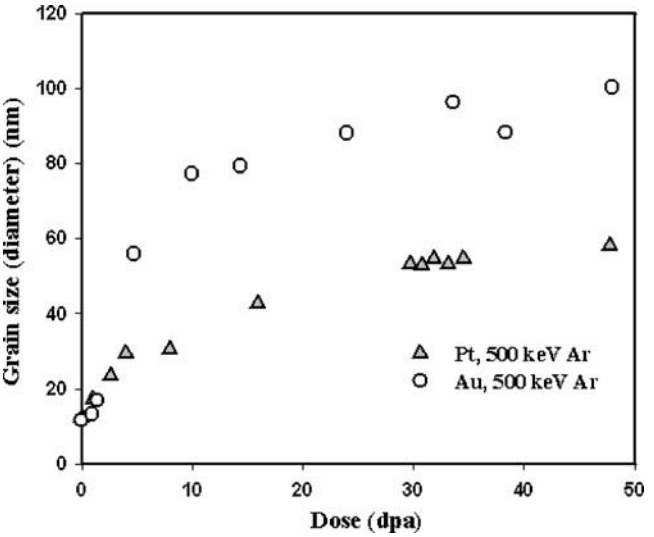

FIG. 11—*Average grain size plotted versus ion dose in dpa for Au and Pt films irradiated with 500 keV Ar ions in the low-temperature regime. Both materials have similar collisional properties but different material properties.*

Similar temperature regimes are seen in other irradiation processes such as atomic diffusion under irradiation and ion beam mixing of multilayers [17]. From our results, we observe that the transition temperature from temperature-independent regime to temperature-dependent regime changes from material to material, but when scaled with the melting temperature of the material in terms of homologous temperatures the transition temperature seems to fall within a common window of temperatures. For our thin films, this transition temperature $\mathcal{T}$ is determined with more or less precision as

$$0.14 < \mathcal{T}_{\mathrm{Zr}} < 0.19,$$

$$0.14 < \mathcal{T}_{\mathrm{Pt}} < 0.23,$$

$$0.03 < \mathcal{T}_{\mathrm{Cu}} < 0.22$$

$$0.04 < \mathcal{T}_{\mathrm{Au}} < 0.22.$$

Thus our results are consistent with the transition from the athermal regime to the thermally-assisted grain growth regime occurring between 0.14 and 0.22 T_m. The previously reported study of ion-irradiation grain growth in Cu reported a transition temperature of about 0.16 T_m [5].

The fact that grain growth also occurs at cryogenic temperatures as low as 20 K indicates that in this regime thermal diffusional processes are not required for grain growth to occur. This indicates that grain growth in this temperature regime is a ballistic driven process, caused by nearly direct collisional impacts at the grain boundaries. In other words, in this temperature regime, the migration of grain boundaries is controlled by intra-cascade processes, and as a result, it depends on the size of the cascades, as discussed below. In fact, it is possible using rate theory [13] to evaluate which regime is operational (recombination-dominated versus sink—dominated). The parameter **E**, defined below, compares the defect losses to vacancy-interstitial recombination (numerator) with the defect losses to fixed-sinks such as voids, dislocations, grain-boundaries, and free surfaces (denominator). $E=(4K_0K_{iv})/(\sum_s k_{is}^2 D_i)(\sum_s k_{vs}^2 D_v)$ where $\mathbf{K_0}$ is the defect formation rate, $\mathbf{K_{iv}}$ is the rate of interstitial-vacancy recombination, $\mathbf{D_v}$ and $\mathbf{D_i}$ are the diffusion coefficients for vacancies and interstitials, k_{is}^2 and k_{vs}^2 are the sink-strengths for interstitials and vacancies, respectively. Calculations of the **E** parameter at the beginning of the irradiation when the grain size is smallest and therefore the sink strength is the highest, show that $\mathbf{E} \gg 1$ for all experiments (but for Au and Cu irradiated at 573 K with 500 keV Ar and 500 keV Kr ions, respectively), which indicates that all these irradiation experiments were conducted in the recombination dominated regime (except for Au and Cu at the highest temperatures investigated).

In the thermally assisted regime, the increase of grain growth rate and of final grain size with increasing temperature may be explained by the larger thermal spike size and the resulting increase in the number of atomic jumps within these thermal spikes. At the highest temperatures, other effects such as subcascade overlap and point defect migration to sinks may also enhance the process.

As far as the purely thermal regime, the observation that for Zr no grain growth occurs under purely thermal conditions at temperatures up to 873 K appears to be at odds with bulk recrystallization temperatures for bulk coarse-grained Zr which are in range of 723–783 K. However, similar observations on the relative thermal stability of nanocrystalline materials are found in the literature [18]. They show that contrary to expectations, grain growth in nanocrystalline materials, prepared by any method, is small compared to that of their bulk counterparts up to a reasonably high (homologous) temperature, although in some instances, abnormal grain growth has been observed. This resistance to grain growth has been attributed to factors such as narrow grain size distribution, equiaxed grain morphology, relatively flat grain boundary configurations, and porosity of the consolidated samples. The effect of pores as Zener drags on the inhibition of grain growth is also evident. One important feature of the structure of nanocrystalline materials is the large number of triple junctions which can inhibit grain growth [19]. Molecular dynamics simulation also suggest that the triple junction drag is important for small grain sizes, low temperatures and high grain-symmetry misorientation [20]. If large enough, ion-induced collision cascades can destroy triple junctions and thus promote grain boundary motion upon rearrangement of the atoms involved in the cascade. This may account for irradiation induced grain growth at low temperatures where triple junctions are the most hindering to grain boundary migration.

On the Grain Size Saturation

As observed on all grain growth curves, the grain growth rate decreases with increasing dose such that the grain size saturates at high doses. The mechanism for this saturation is not totally clear. The thickness of the thin foil is not the limiting factor for grain growth in our case, since for Au and Cu films the final grain size exceeded the thickness of the foil. In fact, grain growth saturation may partly be ascribed to the loss of driving force as the curvature of the grain boundaries becomes smaller. Also, it is likely due to the fact that the probability of cascades hitting the grain boundaries decreases with grain size. The main idea is that grain growth is primarily caused by defect cascades occurring at or near the grain boundaries. Hence, the primary contribution to ion-irradiation induced grain-boundary migration is the direct hitting of the grain boundary with ions. In the early stages of irradiation, grain size is very small, thus the probability of hitting grain boundaries is high; (in fact if the cascade size is bigger than the grain size, the damage region could include entire grains). When the average grain size approaches and finally becomes larger than the diameter of the ion-induced damaged region, the probability of hitting a grain boundary decreased. Using a simple model of a spherical defect cascade of diameter d_c hitting a spherical grain of diameter D, the maximum probability of hitting the grain boundary is given by $3d_c/D$, thus varies inversely with grain diameter. This means the effective displacement rate (i.e., the production rate of displacements directly involved in the grain boundary migration) decreases with increasing grain size, ultimately causing saturation.

Because of the above argument, the saturation grain size depends on the cascade size. As observed in Fig. 6, the saturation grain size depends on the ion type. This is likely due to the different sizes of collision cascades formed by Ar and Kr. Qualitative estimates of (sub)cascade size induced by 600 keV Ar ions and induced by 600 keV Kr ions in Zr performed using SRIM showed that Kr induced cascades in Pt were clearly bigger than those induced by Ar ions. In a study of ion-irradiation induced grain growth in Pd films [6], it was also observed that grain growth in the Pd films irradiated with 560 keV Xe ions was larger than that induced by 185 keV Ar ions and 100 keV Ne ions, leading to the conclusion that the (sub)cascade size may have a direct effect on the final grain size. Although in that study average grain size was plotted versus ion fluence and not dpa, when plotted against dpa the final grain sizes for Xe, Ar, and Ne irradiations in Pd are, respectively, about 60, 40, and 25 nm. In that case the SRIM simulation gives an estimate of sub-cascade size that is quite different among the three, in agreement with the results.

The idea that the primary contribution to ion-irradiation induced grain-boundary migration is ion hits at or near the grain boundary seems to be supported by some molecular dynamics simulation studies [21]. From their molecular dynamics simulations of 5 keV cascades in nanocrystalline nickel with grain sizes of 5 and 10 nm were done, Voegli et al. concluded that if the thermal spike volume is larger than the grain

volume or overlaps the grain boundary area, the ion beam induces grain growth but if the spike volume does not reach the grain boundary area (i.e., cascades are located within the grain volume), no grain growth occurs. This suggests that ion-beam induced grain growth is a direct result of grain-boundary migration inside the thermal spike and therefore inherently different from grain growth observed in thermal annealing simulations.

On the Role of Intrinsic Materials Properties

As mentioned earlier, the difference in grain growth kinetics between Au and Pt means that collisional properties such as the deposited damage energy and the recoil spectra cannot explain alone grain growth kinetics; materials properties such as the melting point and cohesive energy of the target materials must play a determining role too and should be taken into account when modeling grain growth under ion-irradiation. This result agrees with similar observations in the literature. For instance, Liu observed significant variations in grain growth rates among alloys that exhibit similar collisional damage behavior, and suggested that a purely collisional model is inadequate for describing ion-induced grain growth [9]. It was proposed that ion-irradiation induced grain growth may be related to "thermal spike" effects. Liu scaled the ion-induced grain boundary mobility with $F_D^2/\Delta H_{coh}^2$ [9], which was later corrected by Alexander to $F_D^2/\Delta H_{coh}^3$ [2]. The irradiations performed by Alexander in order to verify this dependency were done at room temperature only. Present results on temperature dependence of ion-irradiation induced grain growth suggest that the expression derived by Alexander can only apply in the low-temperature regime where grain growth kinetics is independent of temperature. In the higher-temperature regime a temperature dependent term would have to be added in the expression of the mobility in order to account for the observed dependence of ion-irradiation induced grain growth on temperature which we have reported in this paper.

Conclusions

We have used the Intermediate Voltage Electron Microscope at Argonne to study grain growth in various nanocrystalline metal thin films under in-situ ion irradiation. In this paper, we have presented the main experimental results which are as follows:

1. All samples studied showed a gradual increase in the grain size with ion dose at all temperatures, even at temperatures down to 50 K. At high doses the grain growth saturates. The final grain size may be related to the size of a single subcascade. Grain growth also occurs under purely thermal conditions but is slower than under irradiation.
2. The experiments carried with other materials confirmed the conclusion that similarly to ion beam mixing phenomena, ion-irradiation induced grain growth exhibits three regimes with respect to irradiating temperature:
   (i) a purely thermal regime,
   (ii) a thermally-assisted regime where thermal motion and irradiation effects combine to increase the rate of grain growth caused by either of these mechanisms operating alone, and
   (iii) a low temperature (or "athermal") regime in which ballistic effects of ion irradiation dominate the grain growth process.

The transition temperature between the athermal and thermally assisted regimes depends on the material and can be scaled with its melting temperature; in terms of homologous temperatures, the transition typically occurs at a homologous temperature between 0.14 and 0.22 T_m.

Future work will focus on the modeling of ion-irradiation induced grain growth in the temperature-independent regime where grain boundary mobility is independent of temperature and how this needs to be modified at higher temperatures with a temperature dependent term.

Acknowledgments

The authors would like to thank Bill Drawl of the Materials Research Laboratory at Penn State, and Amelia Liu, Pete Baldo, and Ed Ryan at Argonne National Laboratory for their assistance during the thin film processing and the irradiation experiments. The experimental part of this research was conducted in

the IVEM-Accelerator facility at Argonne National Laboratory, which is supported as a User Facility by the U.S. Department of Energy, Basic Energy Sciences, under contract W-31-109-ENG-38. This study was funded by DOE Nuclear Engineering Education Research program under contract number DOE-NEER (DE-FG07-01ID14115).

References

[1] Wang, P., Thompson, D. A., and Smeltzer, W. W., "Implantation and Grain Growth in Ni Thin Films Induced by Bi and Ag Ions," *Nucl. Instrum. Methods Phys. Res. B*, Vol. 16, No. 2-3, 1986, pp. 288–292.

[2] Alexander, D. E. and Was, G. S., "Thermal-spike Treatment of Ion-induced Grain Growth: Theory and Experimental Comparison," *Phys. Rev. B*, Vol. 47, No. 6, 1993, pp. 2983–2994.

[3] Alexander, D. E., Was, G. S., and Rehn, L. E., "Ion-induced Grain Growth in Multilayer and Co-evaporated Metall Alloy Thin Films," *Nucl. Instrum. Methods Phys. Res. B*, Vol. B59/60, 1991, pp. 462–466.

[4] Alexander, D. E., Was, G. S., and Rehn, L. E., "The Heat-of-mixing Effect on Ion-induced Grain Growth," *J. Appl. Phys.*, Vol. 70, No. 3, 1991, pp. 1252–1260.

[5] Liu, J. C., Li, J., and Mayer, J. W., "Temperature Effect on Ion-irradiation-induced Grain Growth in Cu Thin Films," *J. Appl. Phys.*, 67, No. 5, 1990, pp. 2354–2358.

[6] Liu, J. C., Nastasi, M., and Mayer, J. W., "Ion Irradiation Induced Grain Growth in Pd Polycrystalline thin films," *J. Appl. Phys.*, 62, No. 2, 1987, pp. 423–428.

[7] Atwater, H. A., Thompson, C. V., and Smith, H. I., "Ion-bombardment-enhanced Grain Growth in Germanium, Silicon, and Gold Thin Films," *J. Appl. Phys.*, Vol. 64, 1988, pp. 2337.

[8] Motta, A. T., Paesano, A., Jr., Birtcher, R. C., Teixeira, S. R., and Amaral, L., "Grain Growth in Zr/Fe Multilayers Induced by Ion Irradiation," *Nucl. Instrum. Methods Phys. Res. B*, 1999, pp. 521–525.

[9] Liu, J. C., "Ion Induced Grain Growth and Lateral Thin Film Reactions," Ph.D. in Nuclear Engineering at Cornell University, 1989.

[10] Allen, C. W. and Ryan, E. A., "In-situ Ion Beam Research in Argonne's Intermediate Voltage Electron Microscope," in *Mat. Res. Soc. Symp. Proc.*, 1997, pp. 277–288.

[11] Ziegler, J., Biersack, J. P., and Littmark, U., *The Stopping and Range of Ions in Matter*, Pergamon Press, New York, 1985.

[12] Wang, P., Thompson, D. A., and Smeltzer, W. W., "Implantation of Ni Thin Films and Single Crystals with Ag Ions," *Nucl. Instrum. Methods Phys. Res. B*, Vol. 7-8, Part 1, 1985, pp. 97–102.

[13] Atkinson, H. V., "Theories of Normal Grain Growth in Pure Single Phase Systems," *Acta Metall.*, Vol. 36, No. 3, 1988, pp. 469–491.

[14] Kurtz, S. K. and Carpay, F. M. A., "Microstructure and Normal Grain Growth in Metals and Ceramics. Part I. Theory," *J. Appl. Phys.*, Vol. 51, No. 11, 1980, pp. 5726–5744.

[15] Hillert, M., "On the Theory of Normal and Abnormal Grain Growth," *Acta Metall.*, Vol. 13, No. 3, 1965, pp. 227–238.

[16] Kaoumi, D., Motta, A. T., and Birtcher, R. C., "Grain Growth in Zr–Fe Thin Films During In-situ Ion Irradiation in a TEM," *Nucl. Instrum. Methods Phys. Res. B*, Vol. 242, 2005, pp. 490–493.

[17] Russell, K. C., "The Theory of Phase Stability Under Irradiation," *J. Nucl. Mater.*, Vol. 83, No. 1, 1979, pp. 176–185.

[18] Andrievski, R. A., "Stability of Nanostructured Materials," *J. Mater. Sci.*, Vol. 38, 2003, pp. 1367–1375.

[19] Protasova, S. G., Gottstein, G., Molodov, D. A., Sursaeva, V. G., and Shvindlerman, L. S., "Triple Junction Motion in Aluminum Tricrystals," *Acta Mater.*, Vol. 49, No. 13, 2001, pp. 2519–2525.

[20] Upmanyu, M., Srolovitza, D. J., Shvindlerman, L. S., and Gottstein, G., "Molecular Dynamics Simulation of Triple Junction Migration," *Acta Mater.*, Vol. 50, No. 6, 2002, pp. 1405–1420.

[21] Voegeli, W., Albe, K., and Hahn, H., "Simulation of Grain Growth in Nanocrystalline Nickel Induced by Ion Irradiation," *Nucl. Instrum. Methods Phys. Res. B*, Vol. 202, 2003, pp. 230–235.